Available online at www.pelagiaresearchlibrary.com

Pelagia Research Library

Pelagia Research Library

Advances in Applied Science Research, 2015, 6(8):205-223

Advances in Applied Science Research
Pelagia Research Library

ISSN: 0976-8610
CODEN (USA): AASRFC

Effect of chemical reaction on slip flow of MHD Casson fluid over a stretching sheet with heat and mass transfer

P. Sathies Kumar and K. Gangadhar

Acharya Nagarjuna University Ongole Campus, Ongole, Andhra Pradesh, India

---

ABSTRACT

The two-dimensional magnetohydrodynamic (MHD) stagnation-point flow of electrically conducting non-Newtonian Casson fluid and heat transfer towards a stretching sheet in the presence of mass transfer and chemical reaction is considered. Implementing similarity transformations, the governing momentum, and energy equations are transformed to self-similar nonlinear ODEs and numerical computations are performed to solve those. The investigation reveals many important aspects of flow and heat and mass transfer. If velocity ratio parameter (B) and momentum slip parameter (S), magnetic parameter (M) increase, then the velocity boundary layer thickness becomes thinner. On the other hand, for Casson fluid it is found that the velocity boundary layer thickness is larger compared to that of Newtonian fluid. The magnitude of wall skin-friction coefficient reduces with Casson parameter (β) and also wall skin-friction coefficient increases with S for B<1 whereas decreases with S for B>1. The heat and mass transfer rate is enhanced with increasing values of velocity ratio parameter. The rate of heat transfer is reduces with increasing thermal slip parameter b. Moreover, the presence of chemical reaction reduces concentration.

Keywords: MHD, Casson Fluid, Heat and mass Transfer, Stretching Sheet, Chemical Reaction, Momentum Slip, Thermal Slip.

INTRODUCTION

Due to the increasing importance of non-Newtonian fluids in industry, the stretching sheet concept has more recently been extended to fluids obeying non-Newtonian constitutive equations (Prasad et al. [1]). Khan [2] and Sanjayanand and Khan [3] studied the viscous-elastic boundary layer flow and heat transfer due to an exponentially stretching sheet. Nadeem et al. [4] analysed the flow of Jeffrey fluid and heat transfer past an exponentially stretching sheet. Sahoo and Poncet [5] analysed the effects of slip on third grade fluid past an exponentially stretching sheet. Hayat et al. [6] investigated the Soret and Dufour effects on the magnetohydrodynamic (MHD) flow of the Casson fluid over a stretched surface using homotopy procedure. Bhattacharyya [7] studied the boundary layer stagnation-point flow of Casson fluid and heat transfer towards a shrinking/stretching sheet and concluded that the velocity and thermal boundary layer thicknesses are larger for Casson fluid than that of Newtonian fluid. Ogunsola and Peter [8] studied the effect of thermal radiation on unsteady gravity flow of a power-law fluid with viscous dissipation through a porous medium. Hayat et al. [9] investigated the mixed convection stagnation-point flow of an incompressible non-Newtonian fluid over a stretching sheet under convective boundary conditions. Kirubhashankar et al. [10] investigated the unsteady two-dimensional flow of a non-Newtonian fluid over a stretching porous surface having a prescribed surface temperature. Prasanna Kumar and Gangadhar [11] investigated the momentum and thermal slip flow of MHD Casson fluid over a stretching sheet with viscous dissipation.

Processes involving the mass transfer effect have been recognized as important principally in chemical processing equipment (Cortell [12]). The driving force for mass transfer is the difference in concentration (Hayat et al. [13]). There are some fluids which react chemically with some other ingredients present in them (Raptis and Perdikis

[14]). The transport of mass and momentum with chemical reactive species in the flow caused by a linear stretching sheet is discussed by Andersson et al. [15]. Akyildiz et al. [16] analyzed the transport and diffusion of chemically reactive species over a stretching sheet in a non-Newtonian fluid (fluid of differential type, second grade). Haritha and Sarojamma [17] investigated the effect of variable thermal conductivity and thermal radiation on heat and mass transfer in the MHD flow of a Casson fluid over a porous stretching sheet and concluded that the presence of Casson parameter decreases the wall shear stress due to the fact that the presence of Casson parameter and increase in the value of β reduce velocities and hence the skin friction coefficient reduces and similarly the Nusselt number and Sherwood number reduce. Sarojamma et al.[18] investigated the heat and mass transfer characteristics of a magneto hydrodynamic Casson fluid in a parallel plate channel with stretching walls subject to a uniform transverse magnetic field and this study revealed that with increase in the strength of the magnetic field, the fluid velocity decrease however an enhancement in temperature is noticed and also increase in the Casson parameter the width of the central core region is observed to reduce.

Chemical reaction can be codified as either heterogeneous or homogeneous processes. This depends on whether they occur at an interface or as a single phase volume reaction. The effect of the presence of foreign mass on the free convection flow past a semi-infinite vertical plate was studied by Gebhart et al. [19]. The presence of a foreign mass in air or water causes some kind of chemical reaction. During a chemical reaction between two species, heat is also generated (Byron Bird R.et al. [20]). In most of cases of chemical reaction, the reaction rate depends on the concentration of the species itself. A reaction is said to be first order if the rate of reaction is directly proportional to concentration itself (Cussler [21]). Mukhopadhyay and Gorla [22] obtained the numerical solutions for a class of nonlinear differential equations arising in diffusion of chemically reactive species of a non-Newtonian fluid towards an exponentially stretching surface and considered the first order constructive/destructive chemical reaction and concluded that the increasing values of the Casson parameter is to suppress the velocity field and the concentration is enhanced with increasing Casson parameter. Hunegnaw and Kishan [23] investigated the unsteady magnetohydrodynamic heat and mass transfer flow over stretching sheet embedded in porous medium with variable viscosity and thermal conductivity in presence of viscous dissipation and chemical reaction and concluded that the concentration decreases with the increase of chemical reaction and Schmidt parameter but increases with the increase of unsteadiness parameter. Prasanna kumar and Gangadhar [24] studied the magneto-convective non-Newtonian nanofluid with momentum and temperature dependent slip flow from a permeable stretching sheet with porous medium and chemical reaction.

However, the interactions of magnetohydrodynamic (MHD) stagnation-point flow of electrically conducting non-Newtonian Casson fluid and heat and mass transfer towards a stretching sheet in the presence of chemical reaction, momentum and thermal slip flow is considered. The governing boundary layer equations have been transformed to a two-point boundary value problem in similarity variables and the resultant problem is solved numerically using bvp4c MATLAB solver. The effects of various governing parameters on the fluid velocity, temperature, Concentration, Skin-friction, local Nusselt number and local Sherwood number are shown in figures and analyzed in detail.

2. MATHEMATICAL FORMULATION

Consider the steady two-dimensional incompressible flow of electrically conducting and chemically reactive Casson fluid bounded by a stretching sheet at $y = 0$, with the flow being confined in $y > 0$. It is also assumed that the rheological equation of state for an isotropic and incompressible flow of a Casson fluid can be written as [25, 26]

$$\tau_{ij} = \begin{cases} \left(\mu_B + \dfrac{p_y}{\sqrt{2\pi}}\right) 2e_{ij}, & \pi > \pi_c \\ \left(\mu_B + \dfrac{p_y}{\sqrt{2\pi_c}}\right) 2e_{ij}, & \pi < \pi_c \end{cases} \tag{2.1}$$

where μ_B is plastic dynamic viscosity of the non-Newtonian fluid, p_y is the yield stress of fluid, π is the product of the component of deformation rate with itself, namely, $\pi = e_{ij}e_{ij}$, e_{ij} is the $(i, j)^{th}$ component of the deformation rate, and π_c is critical value of π based on non-Newtonian model. The governing equations of motion, energy equation and spices equation may be written in usual notation as

Continuity equation

$$\frac{\partial u}{\partial x} + \frac{\partial v}{\partial y} = 0 \tag{2.2}$$

Momentum equation

$$u\frac{\partial u}{\partial x}+v\frac{\partial u}{\partial y}=U_s\frac{dU_s}{dx}+\upsilon\left(1+\frac{1}{\beta}\right)\frac{\partial^2 u}{\partial y^2}-\frac{\sigma H_0^2}{\rho}(u-U_s) \tag{2.3}$$

Energy equation

$$\rho c_p\left(u\frac{\partial T}{\partial x}+v\frac{\partial T}{\partial y}\right)=k\frac{\partial^2 T}{\partial y^2}-\frac{\partial q_r}{\partial y} \tag{2.4}$$

Spices equation

$$u\frac{\partial C}{\partial x}+v\frac{\partial C}{\partial y}=D\frac{\partial^2 C}{\partial y^2}-K_0(C-C_\infty) \tag{2.5}$$

The boundary conditions are

$$u=U_w+N_1\upsilon\frac{\partial u}{\partial y}, v=0, T=T_w+D_1\frac{\partial T}{\partial y}, C=C_w \quad \text{at} \quad y=0$$

$$u\to U_s, T\to T_\infty, C\to C_\infty \quad \text{as} \quad y\to\infty \tag{2.6}$$

where u and v are the velocity components in x and y directions, respectively, $U_s = ax$ is the straining velocity of the stagnation-point flow with a (>0) being the straining constant, $U_w = cx$ is the stretching velocity of the sheet with c (>0) being the stretching constant, υ is the kinematic fluid viscosity, ρ is the fluid density, $\beta=\mu_B\sqrt{2\pi_c}/p_y$ is the non-Newtonian or Casson parameter, N_1 is the velocity slip factor, D_1 is the thermal slip factor, σ is the electrical conductivity of the fluid, T is the temperature, C is the concentration, k is the thermal conductivity, c_p is the specific heat, K_0 is the chemical rate constant, q_r is the radiative heat flux, T_w is the constant temperature at the sheet, C_w is the constant concentration at the sheet, T_∞ is the free stream temperature assumed to be constant, C_∞ is the free stream concentration assumed to be constant, and H_0 is the strength of magnetic field applied in the y direction, with the induced magnetic field being neglected. Using the Rosseland approximation for radiation [27], $q_r=\frac{-4\sigma^*}{3k_1}\frac{\partial T^4}{\partial y}$ is obtained, where σ^* the Stefan-Boltzmann constant is and k_1 is the absorption coefficient. We presume that the temperature variation within the flow is such that T^4 may be expanded in a Taylor's series. Expanding T^4 about T_∞ and neglecting higher-order terms we get $T^4=4T_\infty^3T-3T_\infty^4$

Now (2.4) reduces to

$$\rho c_p\left(u\frac{\partial T}{\partial x}+v\frac{\partial T}{\partial y}\right)=k\frac{\partial^2 T}{\partial y^2}+\frac{16\sigma^* T_\infty^3}{3k_1\rho c_p}\frac{\partial^2 T}{\partial y^2} \tag{2.7}$$

We introduce also a stream functions ψ is defined by

$$u=\frac{\partial\psi}{\partial y} \quad \text{and} \quad v=-\frac{\partial\psi}{\partial x} \tag{2.8}$$

Equations (2.3), (2.5) and (2.7) becomes

$$\frac{\partial\psi}{\partial y}\frac{\partial^2\psi}{\partial x\partial y}-\frac{\partial\psi}{\partial x}\frac{\partial^2\psi}{\partial y^2}=U_s\frac{dU_s}{dx}+\upsilon\left(1+\frac{1}{\beta}\right)\frac{\partial^3\psi}{\partial y^3}-\frac{\sigma H_0^2}{\rho}\left(\frac{\partial\psi}{\partial y}-U_s\right) \tag{2.9}$$

$$\rho c_p\left(\frac{\partial\psi}{\partial y}\frac{\partial T}{\partial x}-\frac{\partial\psi}{\partial x}\frac{\partial T}{\partial y}\right)=k\frac{\partial^2 T}{\partial y^2}-\frac{\partial q_r}{\partial y} \tag{2.10}$$

$$\frac{\partial\psi}{\partial y}\frac{\partial C}{\partial x}-\frac{\partial\psi}{\partial x}\frac{\partial C}{\partial y}=D\frac{\partial^2 C}{\partial y^2}-K_0(C-C_\infty) \qquad (2.11)$$

The boundary conditions are

$$\frac{\partial\psi}{\partial y}=U_w+N_1\upsilon\frac{\partial^2\psi}{\partial y^2},\frac{\partial\psi}{\partial x}=0,T=T_w+D_1\frac{\partial T}{\partial y},C=C_w \quad \text{at} \quad y=0$$

$$\frac{\partial\psi}{\partial y}\to U_s,T\to T_\infty,C\to C_\infty \quad \text{as} \quad y\to\infty \qquad (2.12)$$

Now, the dimensionless variable for the stream function is implemented as

$$\psi=\sqrt{c\upsilon}xf(\eta),\theta=\frac{T-T_\infty}{T_w-T_\infty},\phi=\frac{C-C_\infty}{C_w-C_\infty} \qquad (2.13)$$

where the similarity variable η is given by $\eta=y\sqrt{c/\upsilon}$.

Using relation (2.13) and similarity variable, (2.9) to (2.12) finally takes the following self-similar form:

$$\left(1+\frac{1}{\beta}\right)f'''+ff''-f'^2-M\left(f'-B\right)+B^2=0 \qquad (2.14)$$

$$\left(\frac{3R+4}{3R}\right)\theta''+\Pr f\theta'=0 \qquad (2.15)$$

$$\frac{1}{Sc}\phi''+f\phi'-kr\phi=0 \qquad (2.16)$$

The transformed boundary conditions can be written as

$$f=0,f'=1+Sf'',\theta=1+b\theta'',\phi=1 \quad \text{at} \quad \eta=0$$

$$f'\to B,\theta\to 0,\phi=0 \quad \text{as} \quad \eta\to\infty \qquad (2.17)$$

where primes denote differentiation with respect to η, $M=\sigma H_0^2/\rho c_p$ is the magnetic parameter, $b=D_1\sqrt{c/\upsilon}$ is the thermal slip parameter, $B=a/c$ is the velocity ratio parameter, $S=N_1\upsilon\sqrt{c/\upsilon}$ is the momentum slip parameter, $\Pr=\mu c_p/k$ is the Prandtl number $R=k*k_1/4\sigma T_\infty^3$ is the thermal radiation parameter and $kr=K_0/c$ is the chemical reaction parameter,.

The physical quantities of interest are the wall skin friction coefficient C_{fx}, the local Nusselt number Nu_x, and the local Sherwood number Sh_x, which are defined as

$$C_{fx}=\frac{\tau_w}{\rho U_w^2(x)},Nu_x=\frac{xq_w}{\alpha\left(T_w-T_\infty\right)},Sh_x=\frac{xq_m}{D\left(C_w-C_\infty\right)} \qquad (2.18)$$

where τ_w is the shear stress or skin friction along the stretching sheet, q_w is the heat flux from the sheet and q_m is the mass flux from the sheet and those are defined as

$$\tau_w = \left(\mu_B + \frac{p_y}{\sqrt{2\pi}}\right)\left(\frac{\partial u}{\partial y}\right)_{y=0}$$
$$q_w = \alpha\left(\frac{\partial T}{\partial y}\right)_{y=0} \qquad (2.16)$$
$$q_m = D\left(\frac{\partial C}{\partial y}\right)_{y=0}$$

Thus, we get the wall skin friction coefficient C_{fx}, the local Nusselt number Nu_x and the local Sherwood number Sh_x as follows:

$$C_{fx}\sqrt{\mathrm{Re}_x} = \left(1+\frac{1}{\beta}\right) f''(0)$$
$$\frac{Nu_x}{\sqrt{\mathrm{Re}_x}} = -\theta'(0) \qquad (2.17)$$
$$\frac{Sh_x}{\sqrt{\mathrm{Re}_x}} = -\phi'(0)$$

where $\mathrm{Re}_x = \dfrac{U_w x}{\upsilon}$ is the local Reynolds number.

3 SOLUTION OF THE PROBLEM

The set of equations (2.14) to (2.17) were reduced to a system of first-order differential equations and solved using a MATLAB boundary value problem solver called **bvp4c**. This program solves boundary value problems for ordinary differential equations of the form $y' = f(x, y, p), a \le x \le b$, by implementing a collocation method subject to general nonlinear, two-point boundary conditions $g(y(a), y(b), p)$. Here $\boldsymbol{p}$ is a vector of unknown parameters. Boundary value problems (BVPs) arise in most diverse forms. Just about any BVP can be formulated for solution with **bvp4c**. The first step is to write the *ODEs* as a system of first order ordinary differential equations. The details of the solution method are presented in Shampine and Kierzenka[28].

RESULTS AND DISCUSSION

The abovementioned numerical scheme is carried out for various values of physical parameters, namely, the velocity ratio parameter (B), the magnetic parameter (M), the Casson parameter (β), momentum slip parameter (S), thermal slip parameter (b), the Prandtl number (Pr), Schmidt number (Sc), thermal radiation parameter (R), and chemical reaction parameter (kr) to obtain the effects of those parameters on dimensionless velocity and temperature distributions. The obtained computational results are presented graphically in Figures 1-25 and the variations in velocity, temperature and concentration are discussed.

Table 1 Comparison for $-f''(0)$ for $M=S=0$

B	$-f''(0)$				
	Present Study	Prasanna Kumar and Gangadhar [24]	Bhattacharyya [31]	Nazar et al. [30]	Mahapatra and Gupta [29]
0.1	-0.969386	-0.969386	-0.969386	-0.9694	-0.9694
0.2	-0.918107	-0.918107	-0.918107	-0.9181	-0.9181
0.5	-0.667264	-0.667264	-0.667263	-0.6673	-0.6673
2.0	2.017503	2.017503	2.017503	2.0176	2.0175
3.0	4.729282	4.729282	4.729284	4.7296	4.7293

Firstly, a comparison of the obtained results with previously published data is performed. The values of wall skin friction coefficient $f''(0)$ for Newtonian fluid case $(\beta=\infty)$ in the absence of momentum slip parameter and external magnetic field for different values of velocity ratio parameter (B) are compared with those obtained by

Prasanna Kumar and Gangadhar [24], Mahapatra and Gupta [29], Nazar et al. [30] and Bhattacharya [31] in Table 1 in order to verify the validity of the numerical scheme used and those are found in excellent agreement.

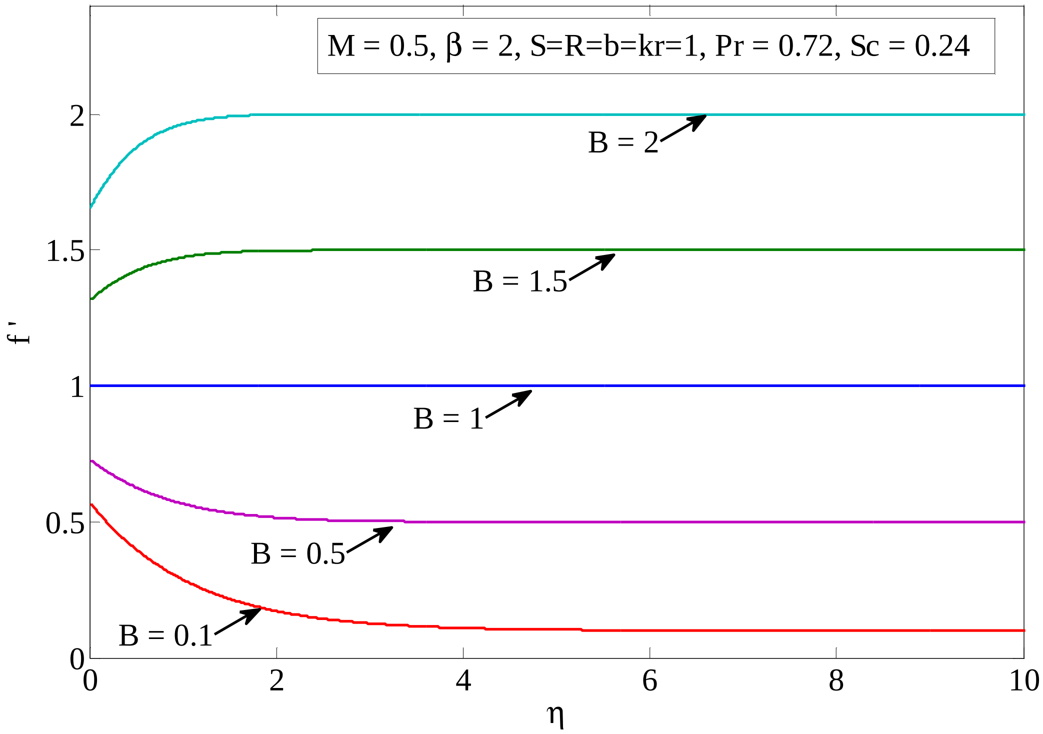

Fig. 1 Velocity for different *B*

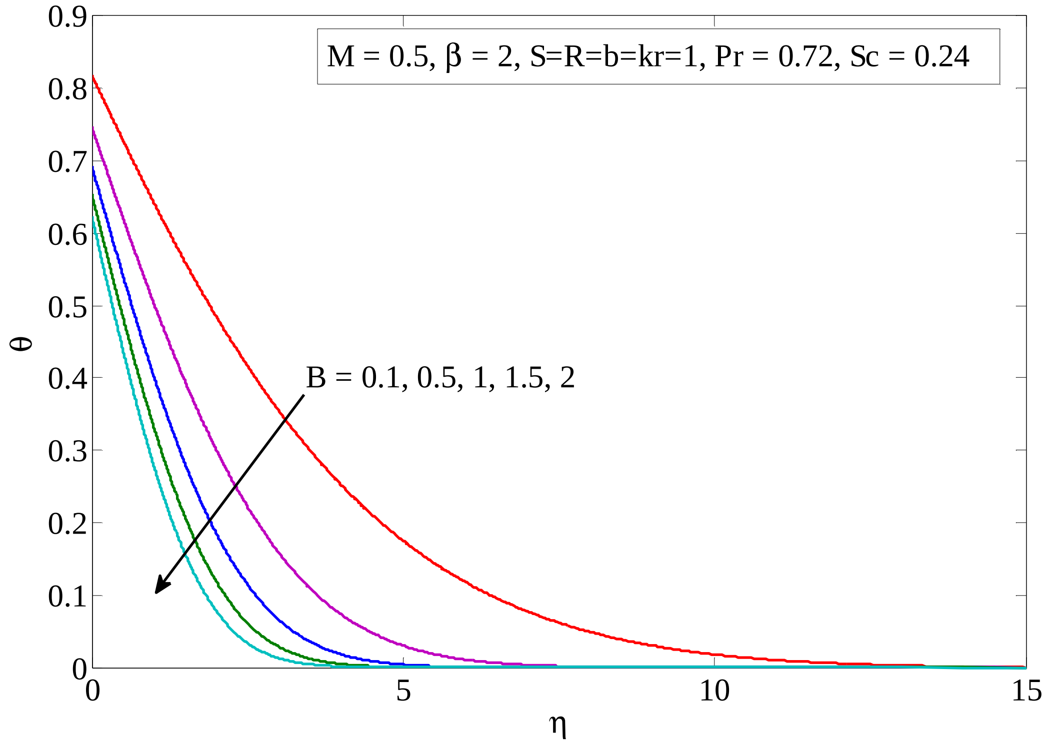

Fig. 2 Temperature for different *B*

The velocity, temperature and concentration profiles for various values of velocity ratio parameter B are plotted in Figs. 1, 2 and 3, respectively. Depending on the velocity ratio parameter, two different kinds of boundary layers are obtained as described by Mahapatra and Gupta [29] for Newtonian fluid. In the first kind, the velocity of fluid inside the boundary layer decreases from the surface towards the edge of the layer (for $B < 1$) and in the second kind the fluid velocity increases from the surface towards the edge (for B > 1). Those characters can be seen from velocity profiles in Fig.1. Also, it is important to note that if B = 1 ($a = c$), that is, the stretching velocity and the straining velocity are equal, then there is no boundary layer of Casson fluid flow near the sheet, which is similar to that of Chiam's [32] observation for Newtonian fluid and also similar to that of Bhattacharya [31]. From Figure 2, it is seen that in all cases thermal boundary layer is formed and the temperature at a point decreases with B, which is similar to that of Bhattacharya [31] observation for Casson fluid. From figure 3, concentration of the fluid decreases with an increasing the velocity ratio parameter.

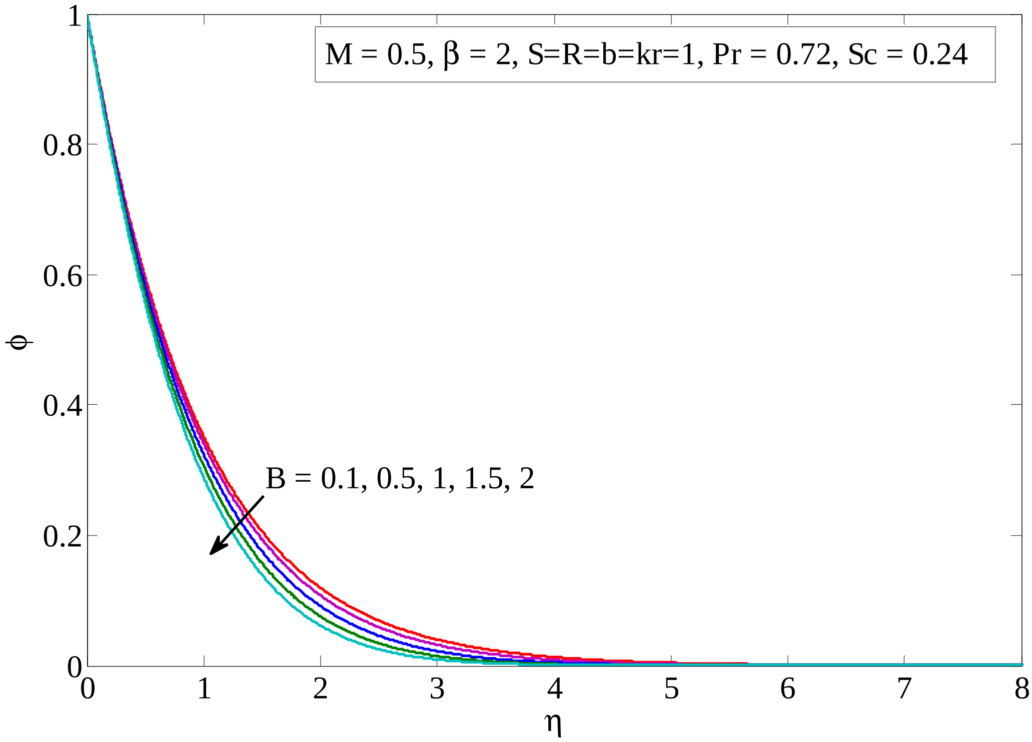

Fig. 3 Concentration for different *B*

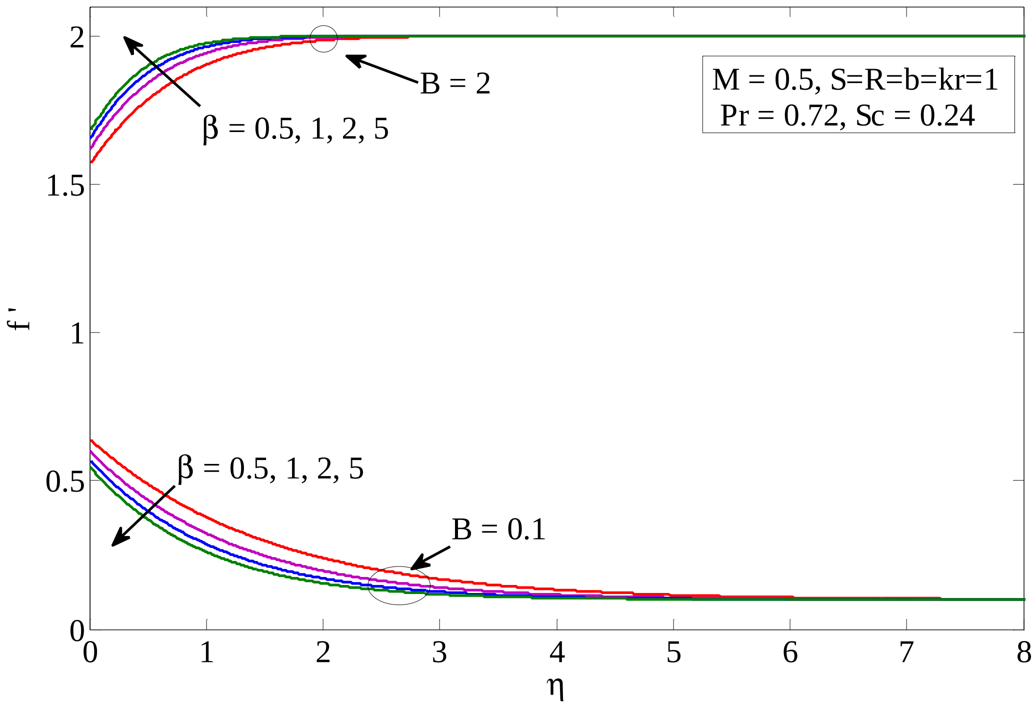

Fig.4 Velocity for different *B* and *β*

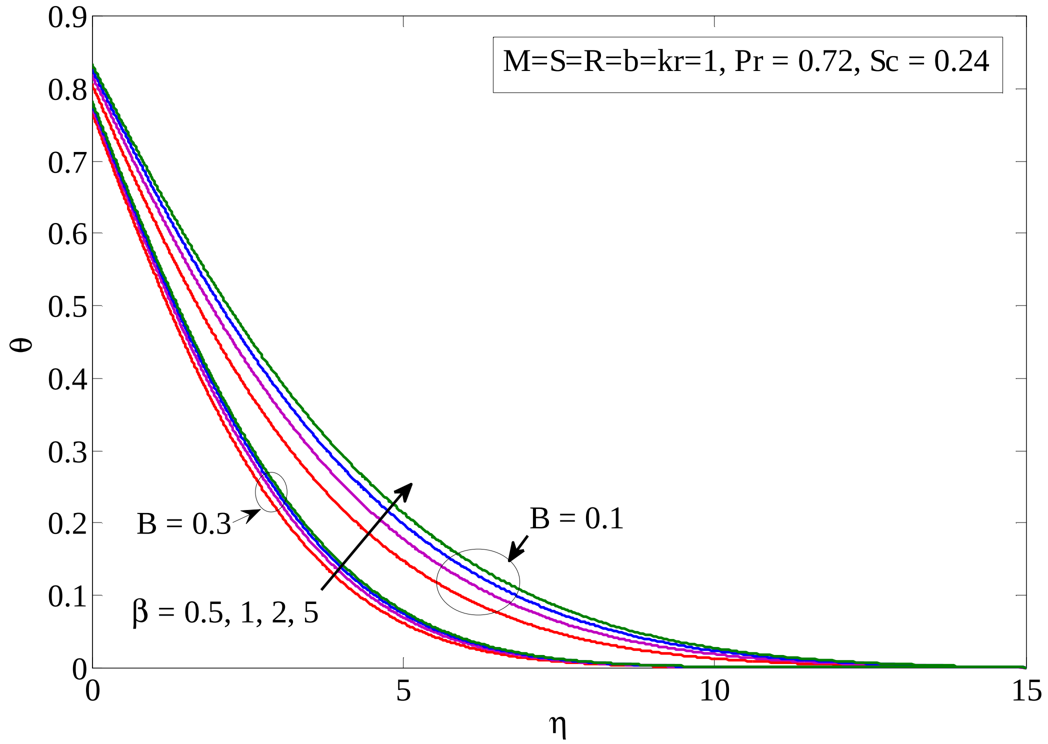

Fig.5 Temperature for different β and B

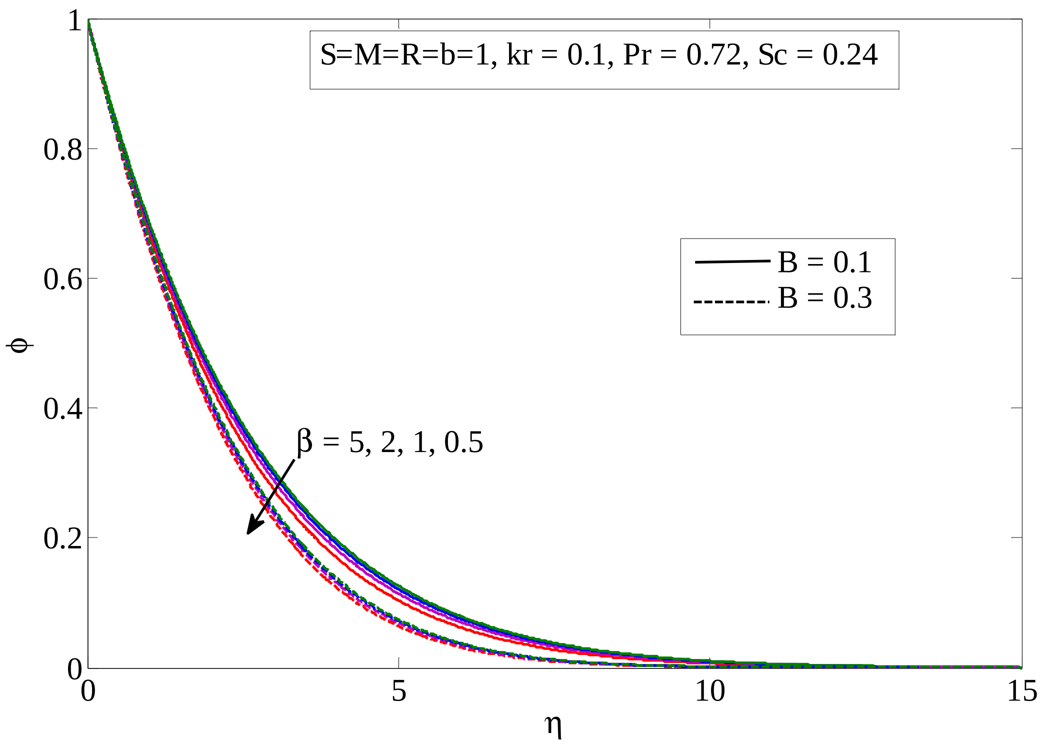

Fig.6 Concentration for different β and B

The effects of Casson parameter β on the velocity, temperature and concentration fields are depicted in Figs. 4, 5 and 6. It is worthwhile to note that the velocity increases with the increase in values of β for B = 2 and it decreases with β for B = 0.1. Consequently, the velocity boundary layer thickness reduces for both values of B. Due to the increase of Casson parameter β, the yield stress p_y falls and consequently velocity boundary layer thickness decreases, these results are similar to that of Bhattacharya [31]. The influences of Casson parameter on the temperature profiles are different in two cases, B = 0.3 and B = 0.1. Temperature and concentration at a point increases with increasing β for both B = 0.1 and B = 0.3.

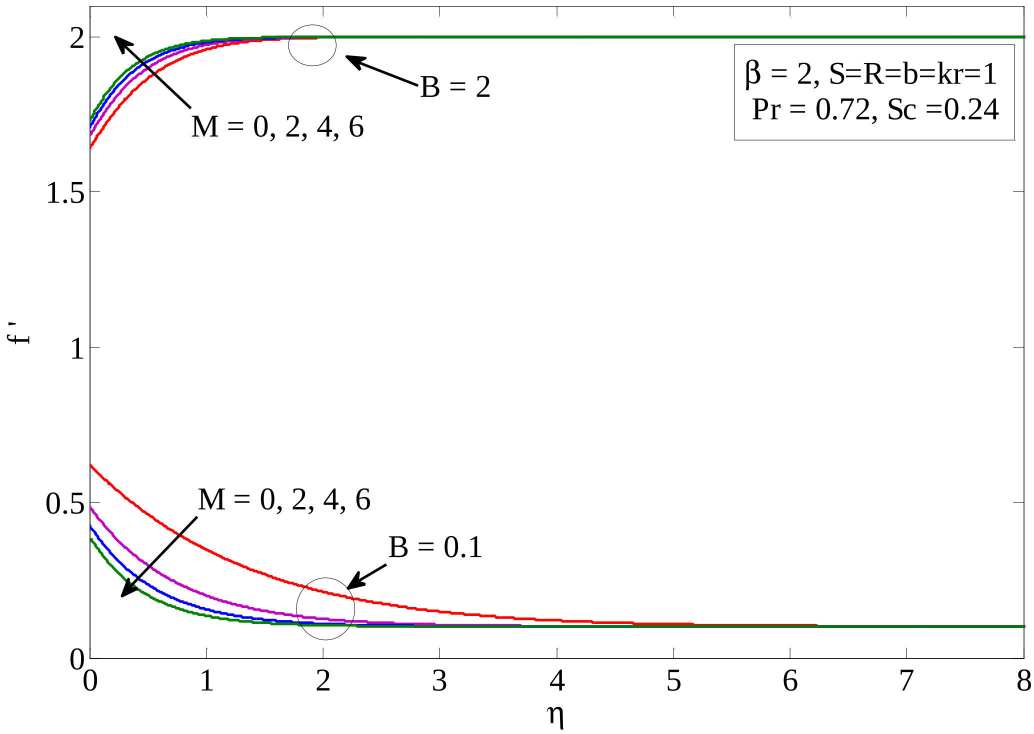

Fig.7 Velocity for different *B* and *M*

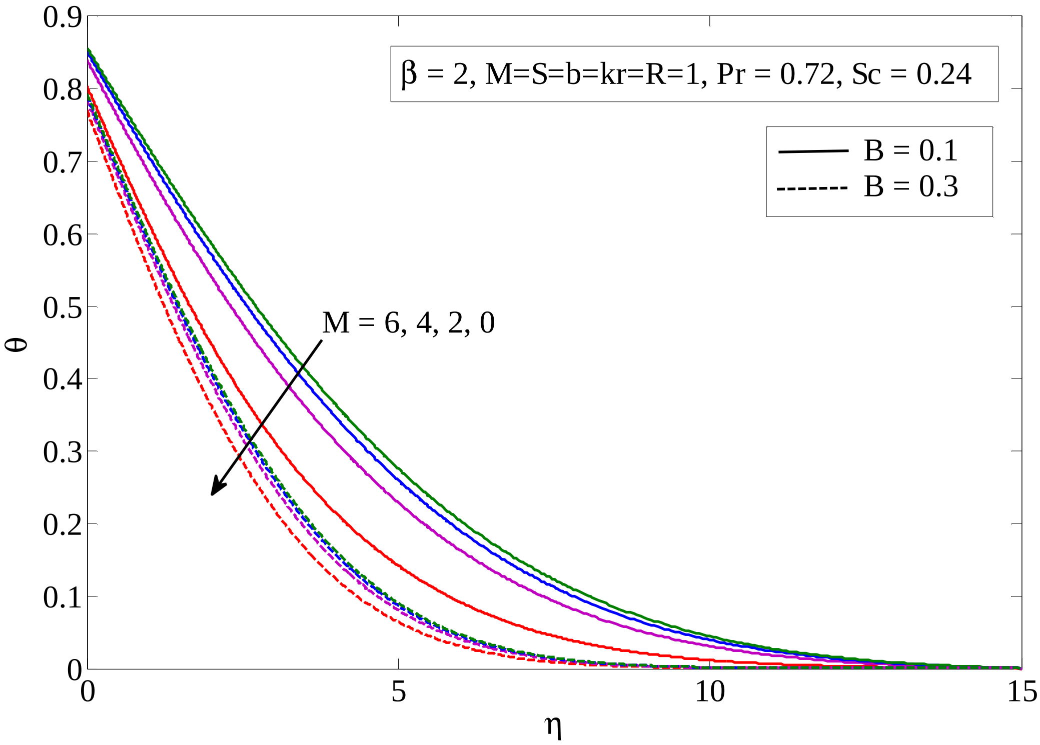

Fig.8 Temperature for different *B* and M

In Figs. 7, 8 and 9, the velocity, temperature and concentration profiles are presented for several values of magnetic parameter M. Similar to that of Casson parameter, due to the increase of magnetic parameter the dimensionless velocity at fixed η increases for B = 2 and for B = 0.1 the velocity decreases. Consequently, for both types of boundary layers, the thickness decreases. The Lorentz force induced by the dual actions of electric and magnetic fields reduces the velocity boundary layer thickness by opposing the transport phenomenon. Also, the temperature and concentration increases with M for both B = 0.1 and B = 0.3.

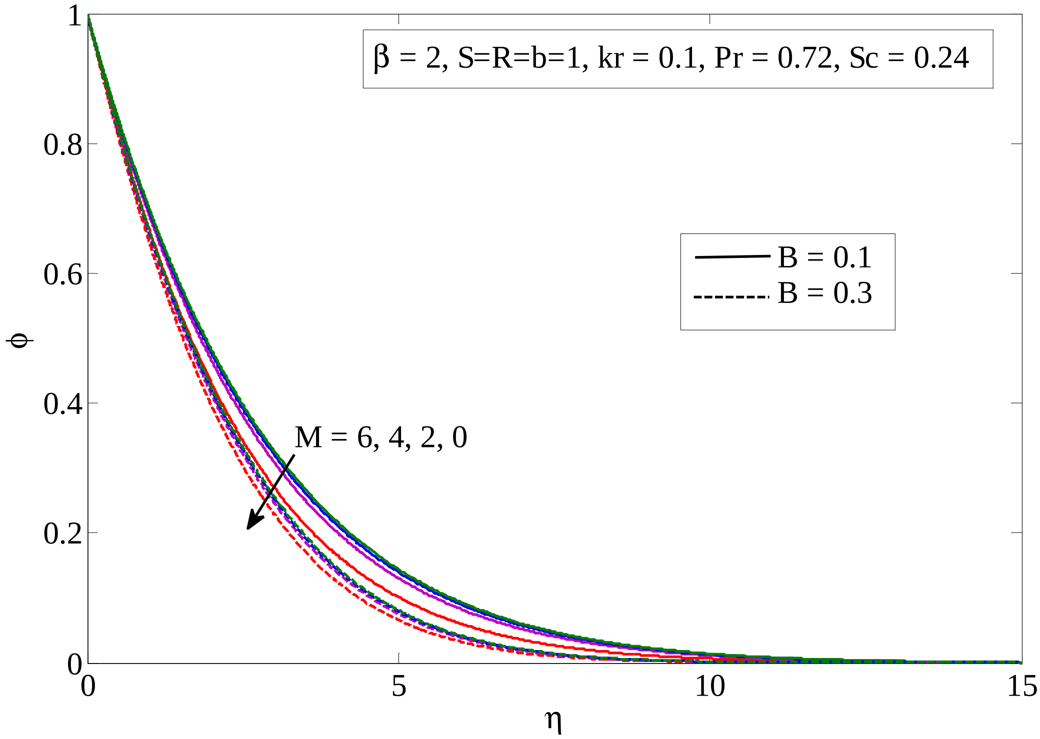

Fig.9 Concentration for different *B* and *M*

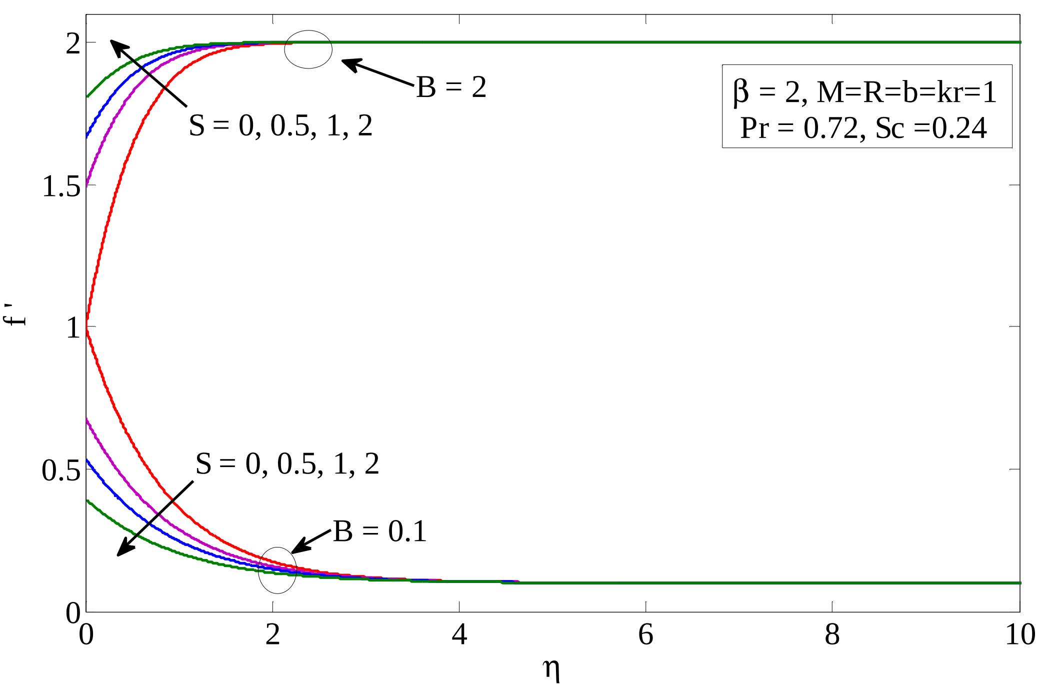

Fig.10 Velocity for different *S* and *B*

The effects of momentum slip parameter S on the velocity, temperature and concentration is depicted in Figs. 10, 11 and 12, respectively. It is worthwhile to note that the velocity increases with the increase in values of S for B = 2 and it decreases with S for B = 0.1. Also, the temperature and concentration decreases with S for both B = 0.1 and B = 0.3.

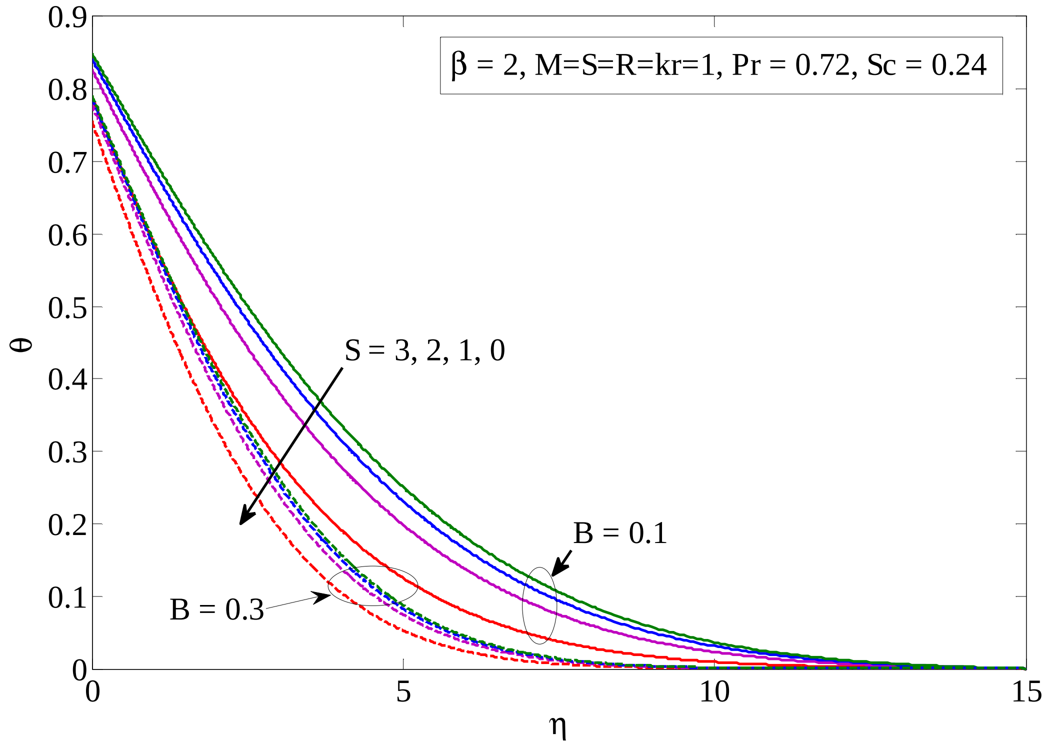

Fig.11 Temperature for different *S* and *B*

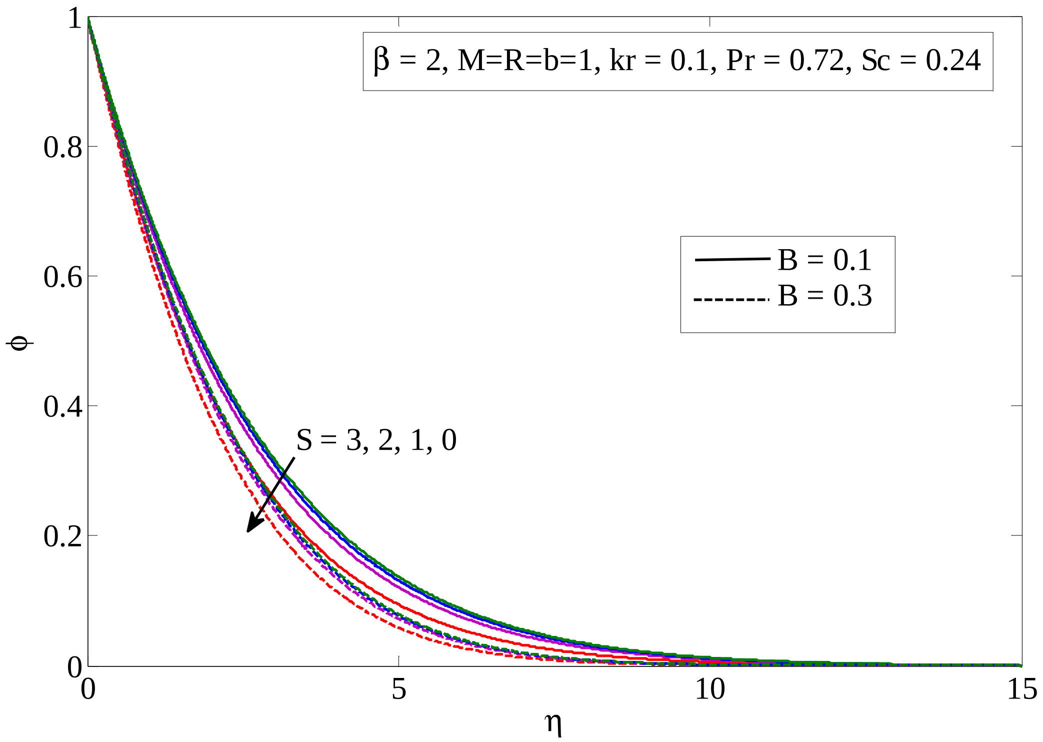

Fig.12 Concentration for different *S* and *B*

The dimensionless temperature profiles for several values of Prandtl number Pr, thermal radiation parameter *R* and thermal slip parameter *b* are exhibited in Figs. 13, 14 and 15, respectively, for two values of B. In both cases (B = 0.1 and 0.3), the temperature decreases with increasing values of Prandtl number, radiation parameter and thermal slip parameter and the thermal boundary layer thickness becomes smaller in all cases. The dimensionless concentration profiles for several values of Schmidt number Sc, chemical reaction parameter kr are exhibited in

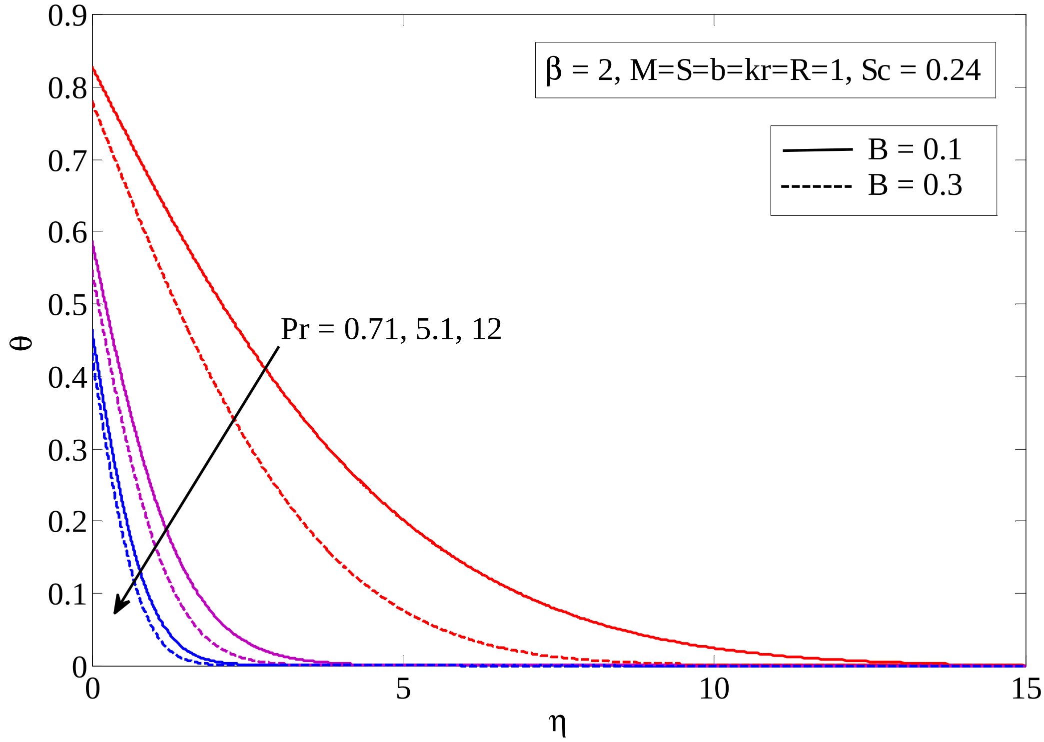

Fig.13 Temperature for different B and *Pr*

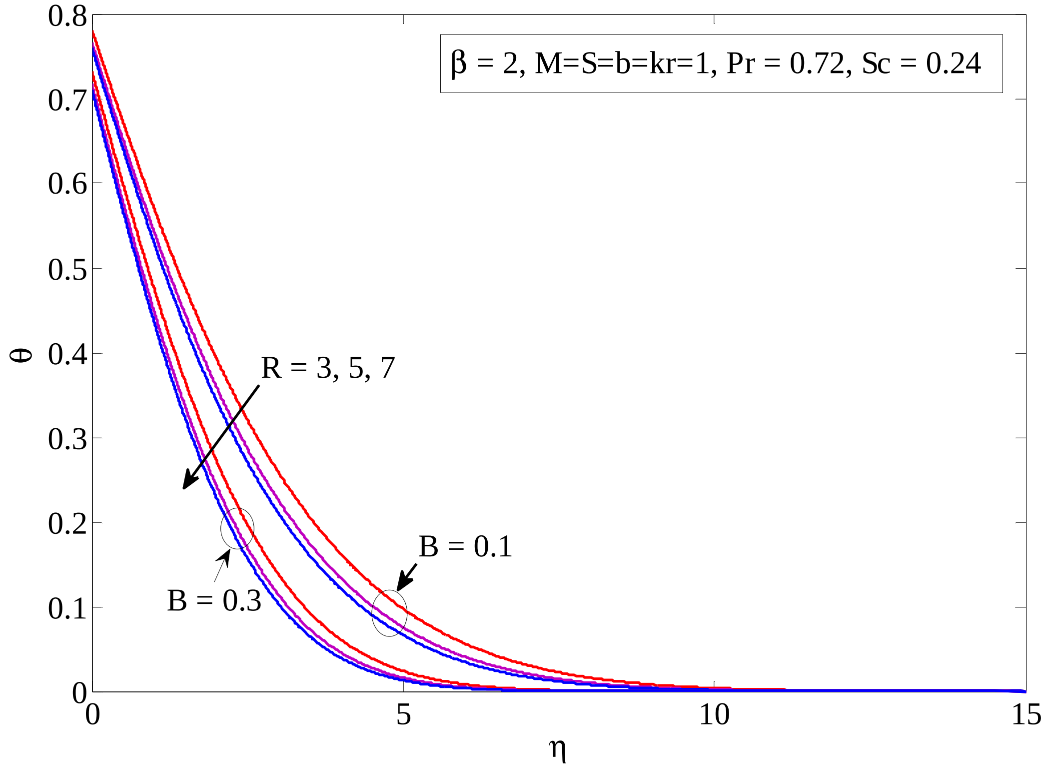

Fig.14 Temperature for different B and *R*

Figs. 16 and 17, respectively, for two values of C. In both cases (B = 0.1 and 0.3), the concentration decreases with increasing values of Schmidt number and chemical reaction parameter and the solutal boundary layer thickness becomes smaller in all cases.

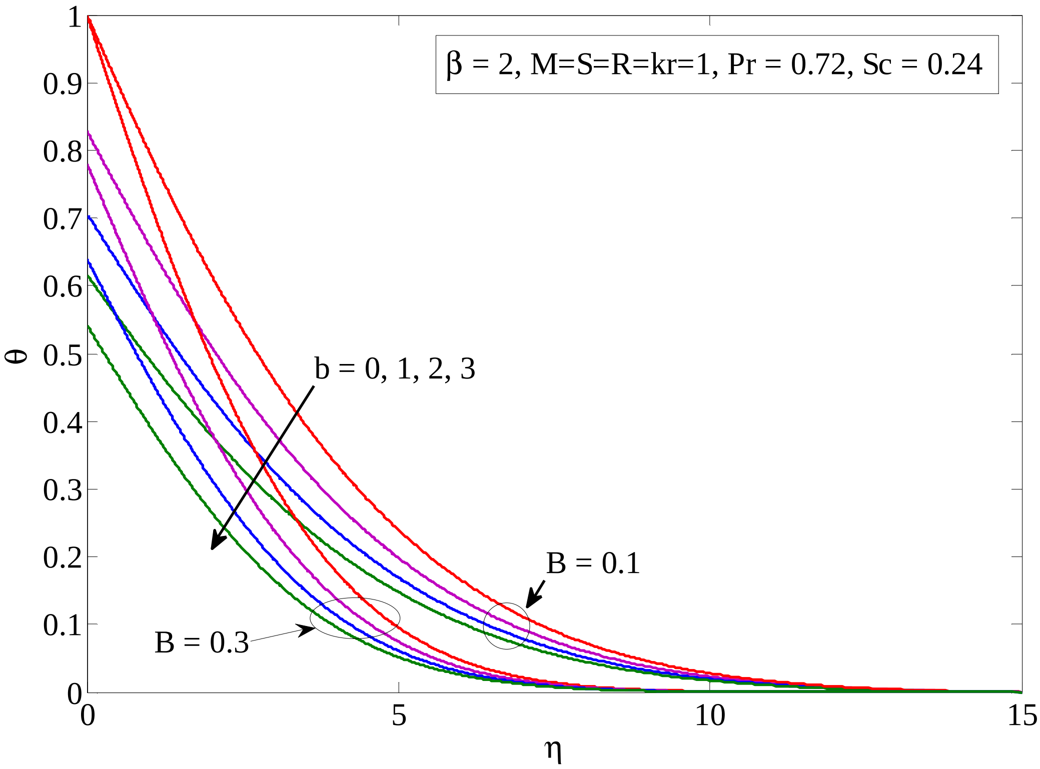

Fig.15 Temperature for different *B* and *b*

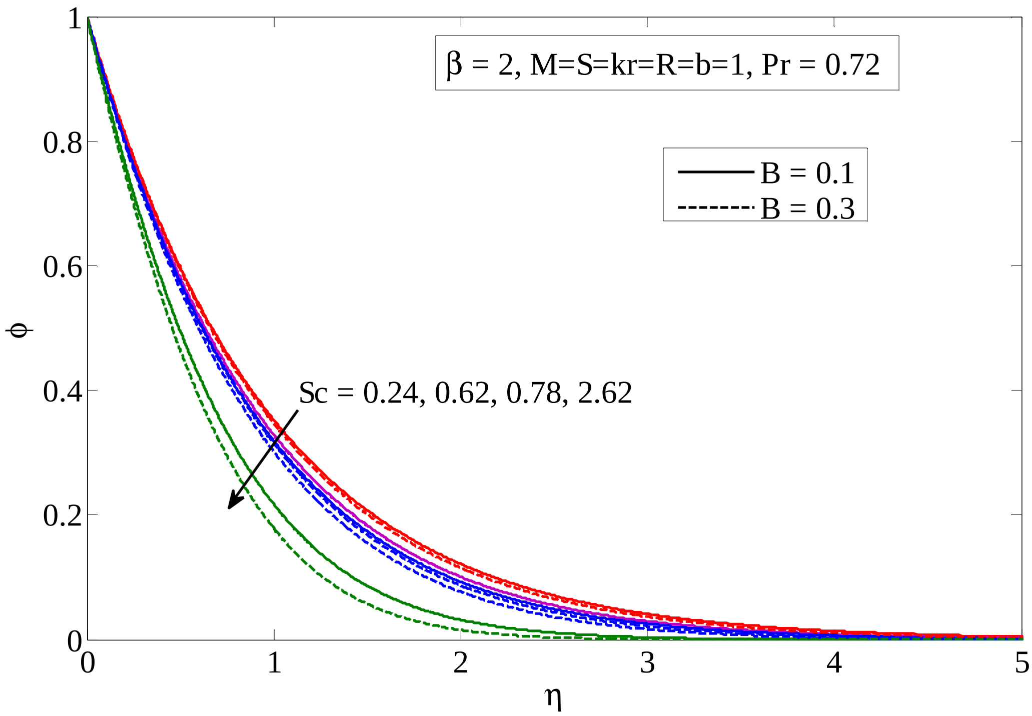

Fig.16 Concentration for different *B* and *Sc*

The physical quantities, the wall skin friction coefficient C_{fx}, local Nusselt number Nu_x, and local Sherwood number Sh_x which have immense engineering applications, are proportional to the values of $\left(1+\frac{1}{\beta}\right)f''(0)$,

$-\theta'(0)$,and $-\phi'(0)$ respectively. The values of $\left(1+\frac{1}{\beta}\right) f''(0)$, $-\theta'(0)$ and $-\phi'(0)$ against the momentum slip parameter S are plotted in Figs.18, 19 and 20, respectively for different values of B. From the figures, it is observed that the magnitude of wall skin friction coefficient, local Nusselt number and local Sherwood number decreases with increasing values of velocity ratio parameter B and the magnitude of wall skin friction coefficient, local Nusselt number and local Sherwood number increases with increasing values of momentum slip parameter S when B < 1, opposite results were found when B > 1.

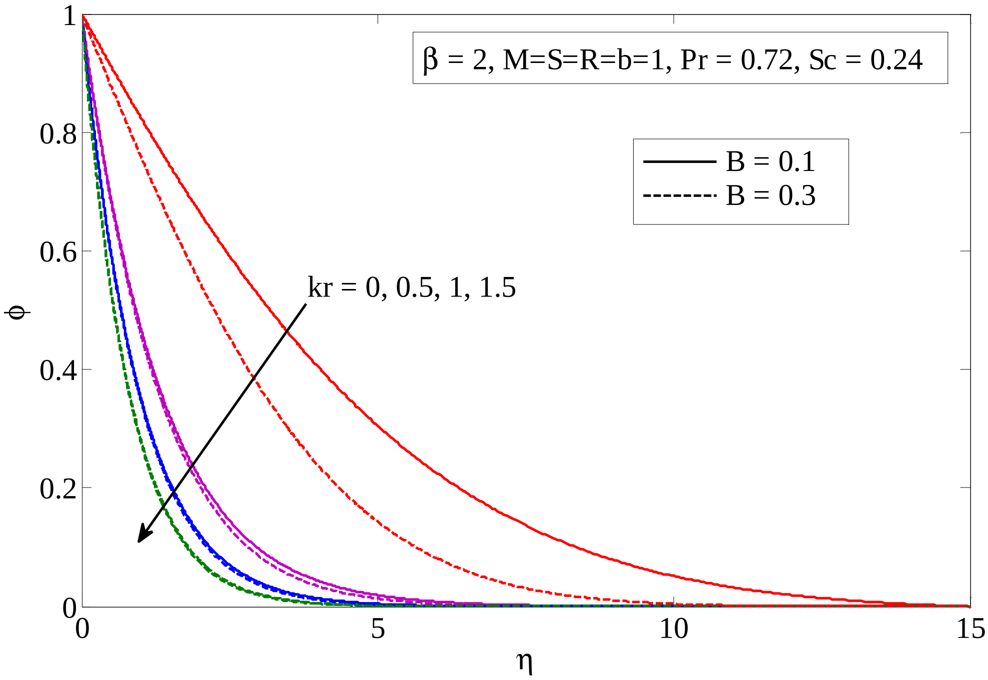

Fig.17 Concentration for different *B* and *kr*

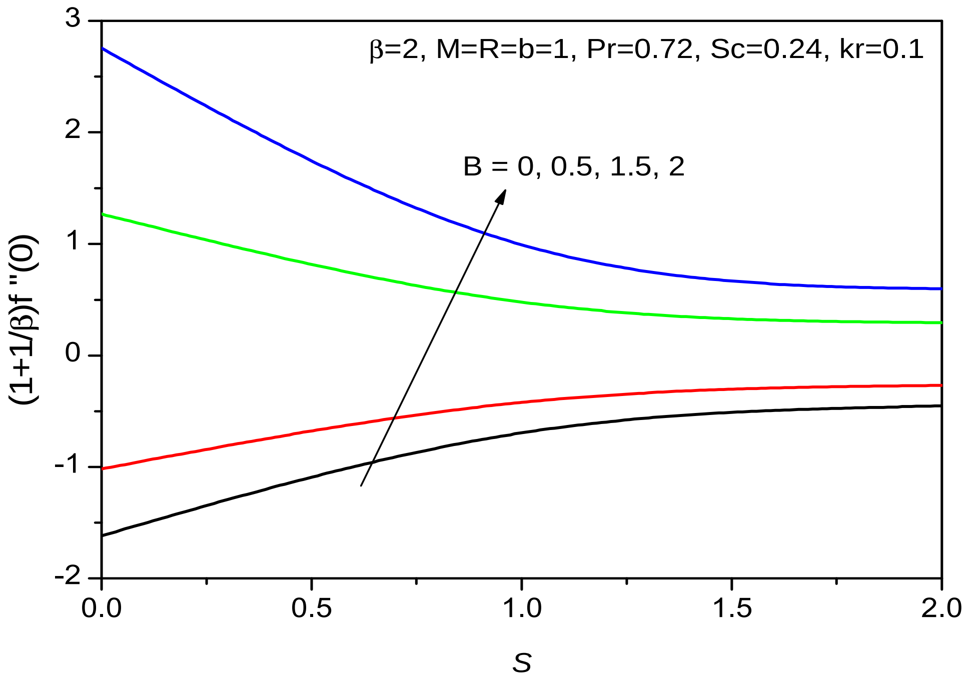

Fig.18 Effect of *S* and *B* on $(1+1/\beta) f''(0)$

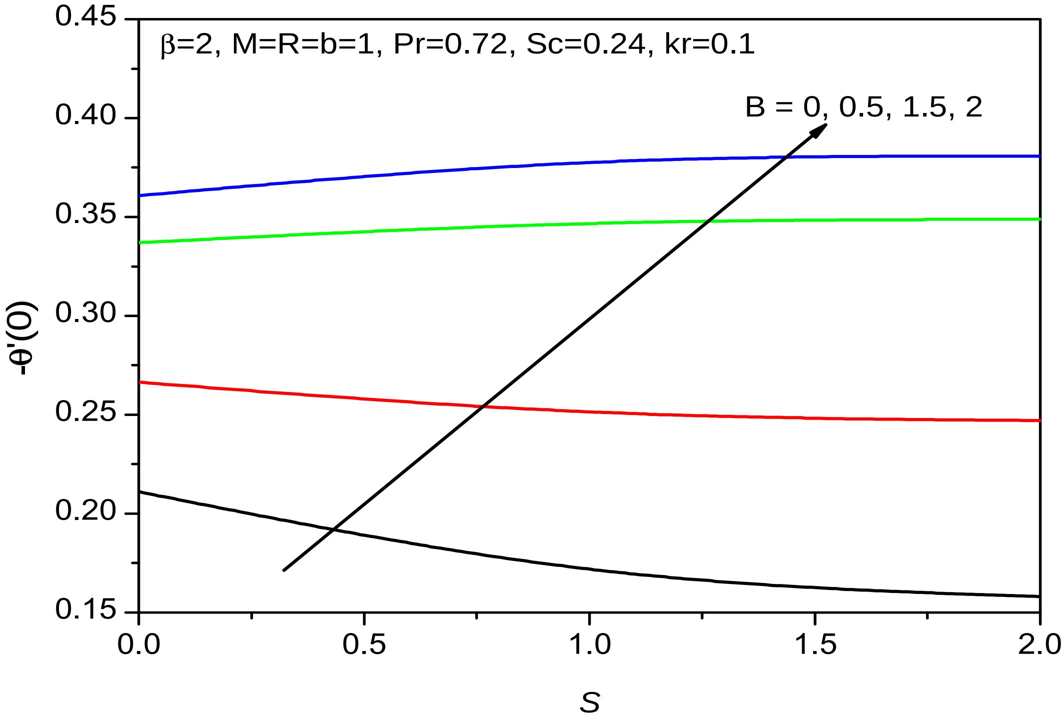

Fig.19 Effect of *S* and *B* on $-\theta'(0)$

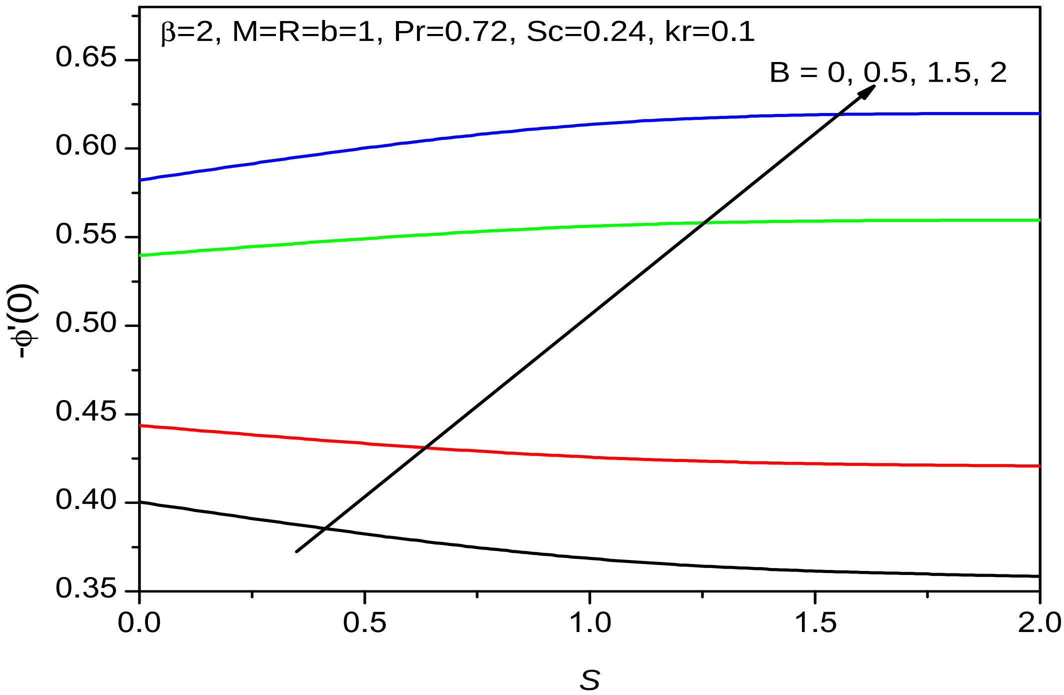

Fig.20 Effect of *S* and *B* on $-\phi'(0)$

The effects of magnetic parameter and Casson parameter on local skin-friction, local Nusselt number and local Sherwood number is shown in figs 21, 22 and 23 respectively. It is noticed that the magnitude of the skin-friction coefficient decrease with the influence of M and increase with raising β. It is also observed that the local Nusselt number and local Sherwood number reduces with the influence of M or β. The local Nusselt number (Figure 24) increases with R, whereas reduced with the influence of thermal slip parameter. The effects of Schmidt number and chemical reaction parameter on local Sherwood number is plotted in Fig. 25. It is noticed that the local Sherwood number decreases with in increases the Schmidt number or chemical reaction parameter.

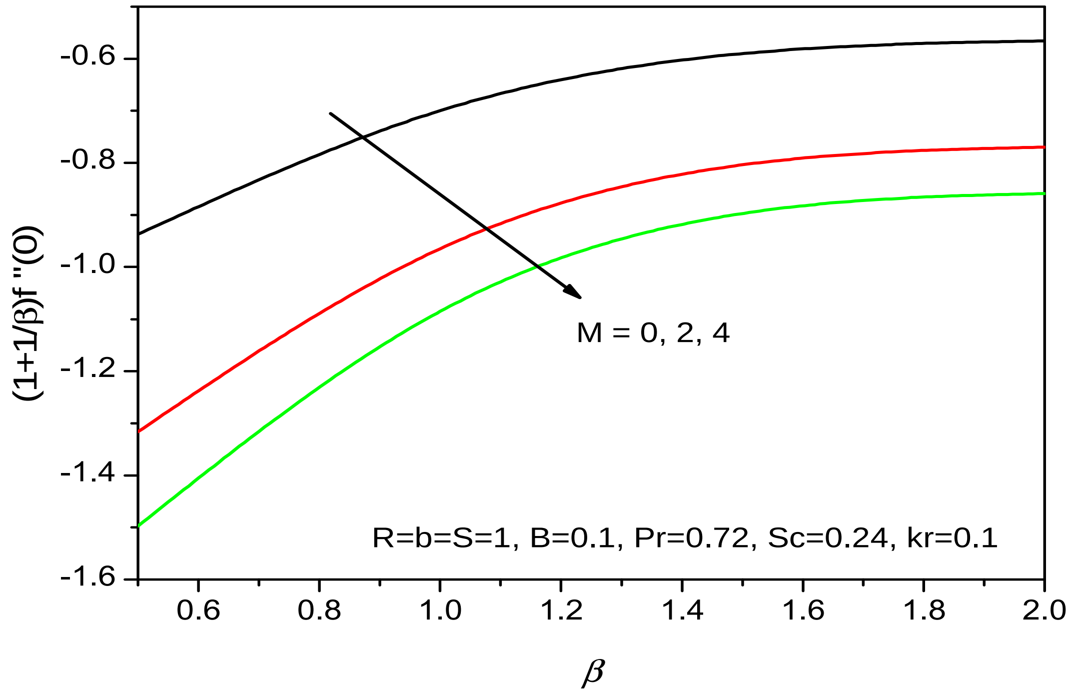

Fig.21 Effect of β and M on $(1+1/\beta)\, f''(0)$

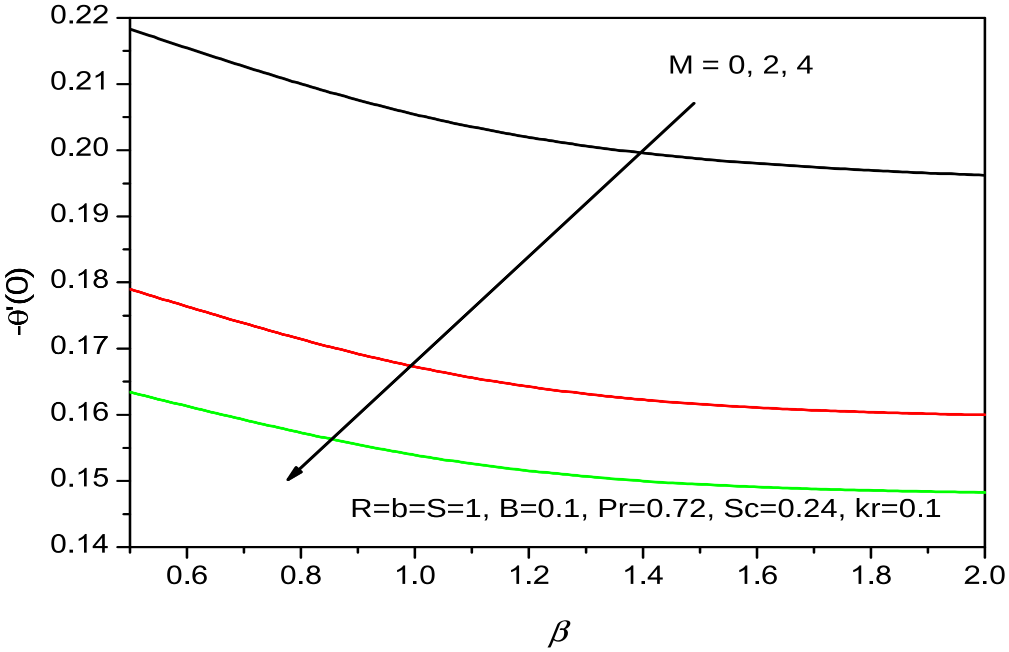

Fig.22 Effect of *M* and β on $(1+1/\beta)\, f''(0)$

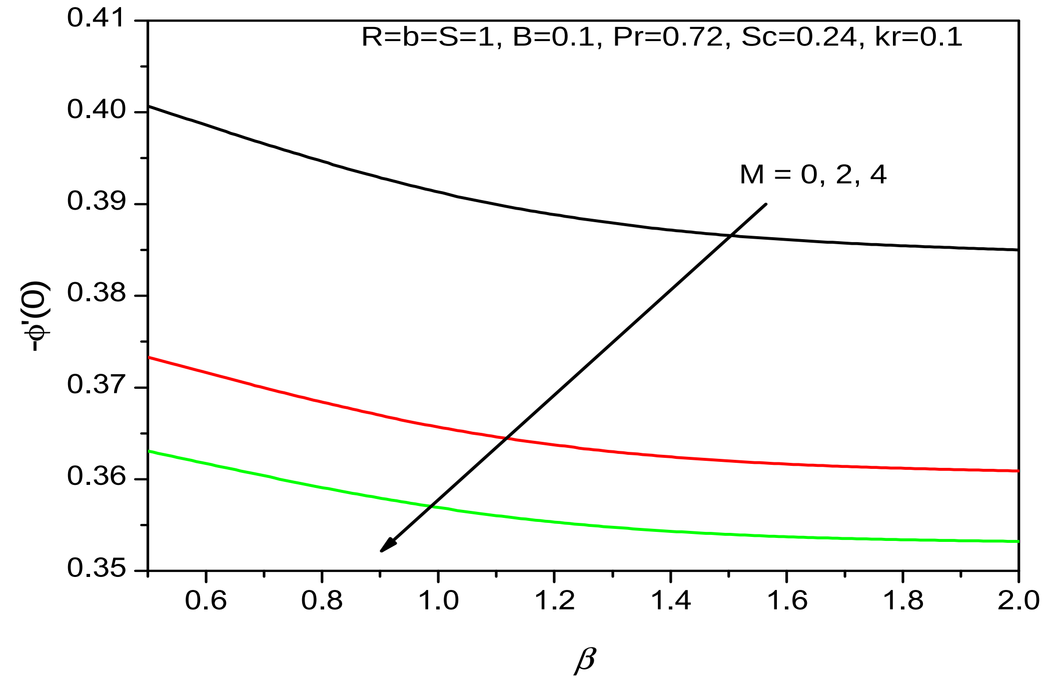

Fig.23 Effect of *M* and *β* on $-\phi'(0)$

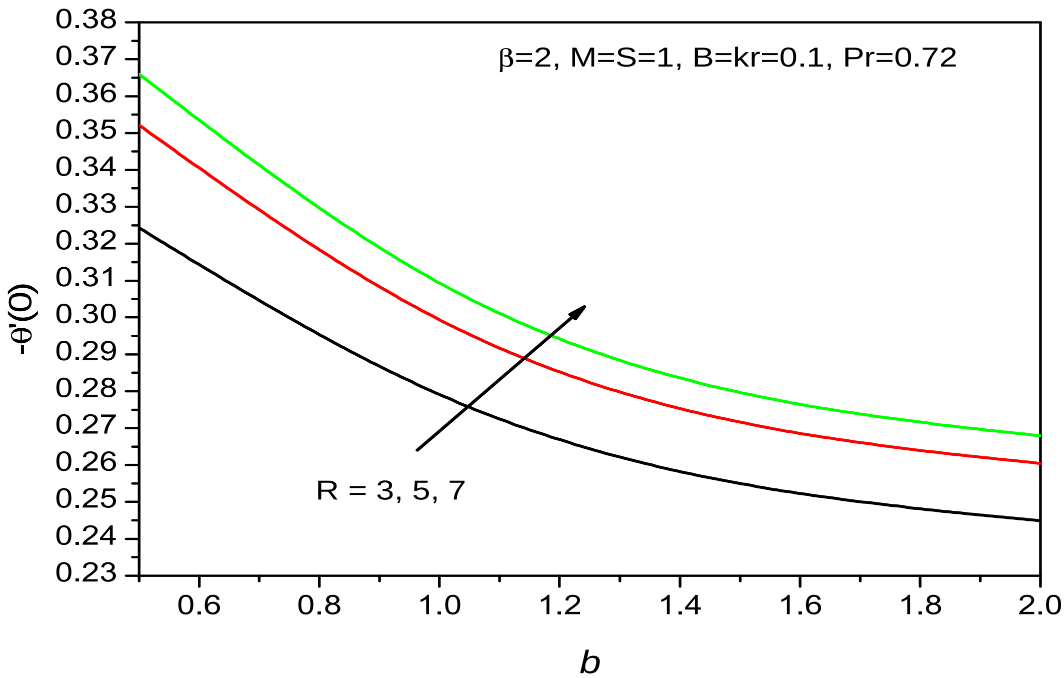

Fig.24 Effect of *b* and *R* on $-\theta'(0)$

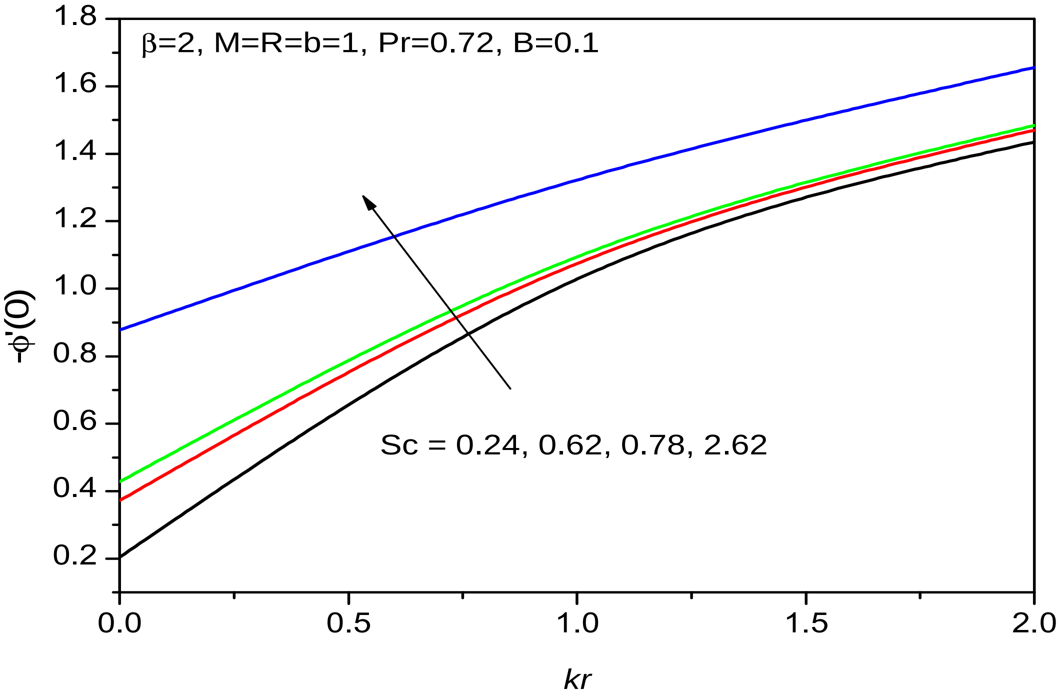

Fig.25 Effect of *Sc* and *kr* on $-\phi'(0)$

CONCLUSION

The MHD stagnation-point flow of Casson fluid and heat and mass transfer over a stretching sheet with radiation are investigated taking into consideration the chemical reaction, momentum and thermal slip effects. Using similarity transformations, the governing equations are transformed to self-similar ordinary differential equations which are then solved using Bvp4c MATLAB solver. From the study, the following remarks can be summarized.

(a) The velocity boundary layer thickness reduces with velocity ratio parameter, magnetic parameter and momentum slip parameter.
(b) The velocity boundary layer thickness for Casson fluid is larger than that of Newtonian fluid.
(c) Temperature and concentration of the fluid increases with an increase Casson parameter.
(d) The magnitude of wall skin-friction coefficient increases with Casson parameter β, but local Nusselt number and local Sherwood number decreases with Casson parameter β.

REFERENCES

[1] Prasad K. V., Abel S., and Datti P. S., (**2003**), *Int. J. of Non-Linear Mech*., Vol.38, pp.651 – 657.
[2] Khan S. K., (**2006**), *Int. J. of Appl. Mech. and Engng*., Vol.11, Vol.321-335.
[3] Sanjayanand E., and Khan S. K., (**2006**), *Int. J. of Ther. Sci*., Vol.45, pp.819-828.
[4] Nadeem S., Zaheer S., and Fang T., (**2011**), *Numer. Algor.*, DOI 10.1007/s11075-010-9423-8.
[5] Sahoo B., and Poncet S., (**2011**), *Int. J. of Heat and Mass Transfer*, Vol54, pp.5010–5019.
[6] Hayat T., Shehzad S. A., and Alsaedi A., (**2012**), *Appl. Math. Mech. -Engl.* Ed., Vol.33(10), pp.1301–1312.
[7] Krishnendu Bhattacharyya, (**2013**), Boundary layer stagnation-point flow of casson fluid and heat transfer towards a shrinking/stretching sheet, Frontiers in Heat and Mass Transfer (FHMT), Vol.4, 023003.
[8] Ogunsola A.W., Peter B.A., (**2014**), *IOSR Journal of Computer Engineering* (IOSR-JCE) e-ISSN: 2278-0661, p-ISSN: 2278-8727, Vol. 16, Issue 4, pp. 18-23.
[9] Hayat T., Shehzad S. A., Alsaedi A., Alhothuali M. S., (**2012**), *Chin. Phys. Lett*. Vol. 29, No. 11, 114704.
[10] Kirubhashankar C. K., Ganesh S., and Mohamed Ismail A., (**2015**), *Applied Mathematical Sciences*, Vol. 9, No. 7, pp.345 - 351
[11] Prasanna Kumar, T., and Gangadhar, K., (**2015**), *International Journal Of Modern Engineering Research* (IJMER), Vol. 5, Iss. 5, pp.24-37.

[12] Cortell R., (**2007**), *Chem. Engng. and Process*., Vol.46, pp.721–728.
[13] Hayat T., Awais M., Qasim M., and Hendi A. A., (**2011**), *Int. J. of Heat and Mass Transfer*, Vol. 54, pp.3777-3782.
[14] Raptis A., and Perdikis C., (**2006**), *Int. J. of Non-Linear Mech*., Vol.41, pp.527 – 529.
[15] Andersson H. I., Hansen O. R., and Holmedal B., (**1994**), *Int. J. Heat Mass Transfer*, Vol.37, pp.659-664.
[16] Akyildiz F. T., Bellout H., and Vajravelu K., (**2006**), *J. Math. Anal. Appl*., Vol.320, pp.322–339.
[17] Haritha A. and Sarojamma G., (**2014**), *International Journal of Applied Mathematics*, ISSN: 2051 – 5731, Vol. 29, pp. 1287 – 1293.
[18] Sarojamma G., Vasundhara B., and Vendabai K., (**2014**), *International Journal of Scientific and Innovative Mathematical Research (IJSIMR)*, Vol. 2, pp. 800-810 ISSN 2347-307X (Print) & ISSN 2347-3142 (Online).
[19] Gehart B., Pera L., (**1971**), *International Journal of Heat Mass Transfer*, Vil.14, pp.2025-2050.
[20] Byron Bird R, Warren E Stewart, Edwin N. Lightfoot, (**1992**), Transport phenomena, John Wiley and Sons, New York.
[21] Cussler E.L., (**1988**), Diffusion Mass Transfer in Fluid Systems, Cambridge University Press, London, UK.
[22] Mukhopadhyay Swati and Rama Subba Reddy Gorla, (**2014**), *Thermal Energy and Power Engineering*, Vol. 3, pp. 216-221.
[23] Hunegnaw D., and Kishan N., (2014), *American Chemical Science Journal*, Vol.4(6), pp. 901-917.
[24] Prasanna kumar, T., and Gangadhar, K., (**2015**), Magneto-convective non-Newtonian nanofluid with momentum and temperature dependent slip flow from a permeable stretching sheet with porous medium and chemical reaction, e-ISSN: 2278-5728, p-ISSN: 2319-765X. Vol. 11, Issue 3 Ver. I, pp. 01-18.
[25] Bhattacharyya, K., Hayat, T., and Alsaedi, A., (**2013**). “Exact solution for boundary layer flow of Casson fluid over a permeable stretching/shrinking sheet,” *Zeitschrift f¨ur Angewandte Mathematik und Mechanik*.
[26] Nakamura, M., and Sawada, T., (**1988**), *Journal of Biomechanical Engineering*, vol. 110, no. 2, pp. 137–143.
[27] Brewster, M. Q., (**1972**), *Thermal Radiative Transfer Properties*, John Wiley and Sons.
[28] Shampine, L. F. and Kierzenka, J. (**2000**), “Solving boundary value problems for ordinary differential equations in MATLAB with bvp4c,” Tutorial Notes.
[29] Mahapatra, T. R., and Gupta, A. S., (**2002**), *Heat and Mass Transfer*, vol. 38, no. 6, pp. 517–521, 2002.
[30] Nazar, R., Amin, N., Filip, D., and Pop, I., (**2004**), *International Journal of Engineering Science*, vol. 42, no. 11-12, pp. 1241–1253.
[31] Bhattacharyya Krishnendu, (**2013**), *Journal of Thermodynamics*, Volume **2013**, Article ID 169674, 9 pages
[32] Chiam, T. C., (**1994**), *Journal of the Physical Society of Japan*, vol. 63, no. 6, pp. 2443-2444, 1994